Ulcerative colitis-associated colorectal cancer arises in a field of short telomeres, senescence, and inflammation

Rosa Ana Risques[1,*], **Lisa A. Lai**[2,*], **Cigdem Himmetoglu**[1], **Anoosheh Ebaee**[1], **Lin Li**[3], **Ziding Feng**[3], **Mary P. Bronner**[4], **Bassel Al-Lahham**[5], **Kris V. Kowdley**[6], **Keith D. Lindor**[7], **Peter S. Rabinovitch**[1,3], and **Teresa A. Brentnall**[2]

[1]Department of Pathology, University of Washington, Seattle, WA

[2]Department of Medicine and Division of Gastroenterology, University of Washington, Seattle, WA

[3]Division of Public Health Sciences, Fred Hutchinson Cancer Research Center, Seattle, WA

[4]Department of Anatomic Pathology, Cleveland Clinic, Cleveland, OH

[5]Digestive Disease Institute, Cleveland Clinic, Cleveland, OH

[6]Virginia Mason Medical Center, Seattle, WA

[7]Division of Gastroenterology and Hepatology, Mayo Clinic College of Medicine, Rochester, NY

Abstract

Inflammation plays a role in the progression to cancer and it is linked to the presence of senescent cells. Ulcerative colitis (UC) is a chronic inflammatory disease that predisposes to colorectal cancer. Tumorigenesis in this setting is associated with telomere shortening that can be observed in the non-dysplastic epithelium of UC patients with high-grade dysplasia (HGD) or cancer (UC Progressors). We hypothesized that a pre-neoplastic field of inflammation, telomere shortening, and senescence underlies tumor progression in UC Progressors. Multiple biopsies of varying histological grade were collected along the colon of 9 UC Progressors and analyzed for telomere length, DNA damage, senescence, p53, p16, and chronic and acute inflammation. Twenty biopsies from 4 UC non-Progressors and 21 biopsies from control individuals without UC were also analyzed. Short telomeres and increased DNA damage, senescence, and infiltrating leukocytes were observed in biopsies located less than 10 cm from HGD or cancer. Low-grade dysplasia had the shortest telomeres along with the highest levels of senescence and infiltrating leukocytes, whereas HGD biopsies showed the opposite pattern. p16 and p53 expression was low in non-dysplastic biopsies, but progressively increased in LGD and HGD. Additionally, high levels of infiltrating leukocytes were associated with telomere shortening, senescence, and reduced p53 expression. These results suggest that dysplasia arises in a pre-neoplastic field of chronic inflammation which leads to telomere shortening, DNA damage, and senescence. Our findings argue that senescence acts as a tumor suppressor mechanism that is abrogated during the transition from LGD to HGD in ulcerative colitis.

Keywords

ulcerative colitis; telomere length; inflammation; senescence; colon

Correspondence should be addressed to: Rosa Ana Risques, Department of Pathology, Box 357705, 1959 NE Pacific St., K-081 HSB, University of Washington, Seattle, WA 98195-7705, Phone: 206.543.5337, Fax: 206.616.8271, rrisques@u.washington.edu.
*Both authors contributed equally

Introduction

Ulcerative colitis (UC) is an inflammatory bowel disease that predisposes to the development of colorectal cancer. The sequence of pathological changes observed in the colonic epithelium progresses from non-dysplastic (no pathological abnormalities) to dysplasia (indefinite (IND), low-grade dysplasia (LGD), and high-grade dysplasia (HGD)) and to cancer. These neoplastic changes can be widespread and/or multifocal. Molecular abnormalities, including telomere shortening, chromosomal instability, p53 alterations, and aneuploidy, underlie these neoplastic changes, in a multistep process of cancer progression (1). Remarkably, these molecular alterations are found not only in neoplasia, but also in histologically normal tissue, indicating that they precede the development of dysplasia (2). The presence of this "field effect" is common in epithelial carcinogenesis (3). In UC, we and others have reported a field effect for aneuploidy, p53 mutations, and clonal chromosomal abnormalities in normal epithelium adjacent to dysplasia (4-7) or even throughout the whole colon (8). However, the cellular and molecular mechanisms that underlie this field effect are poorly understood.

Telomeres shorten as a consequence of cell replication as well as oxidative damage (9). We have previously demonstrated that there is an accelerated shortening in UC colonocytes compared to normal individuals (10) and that telomere shortening is one of the initial triggers of UC tumorigenesis, which leads to chromosomal instability through cycles of bridge-breakage- fusion (11). Thus, we hypothesized that UC is a disease of accelerated colon aging, in which chronic inflammation leads to telomere shortening and, eventually, to cancer progression. Evidence for an association between chronic inflammation and cancer risk come from the fact that the duration, extent and severity of inflammation are risk factors for neoplasia in UC (12), and that anti-inflammatory medications reduce that risk (13). Several studies suggest that reactive oxygen species produced by activated neutrophils and macrophages can contribute to tumor initiation by causing DNA damage (reviewed in (14,15)). However, the mechanistic link between telomere shortening, inflammation, and neoplastic progression has not been fully explored.

In the presence of proficient cellular checkpoints, the outcome of telomere shortening is not chromosomal instability, but senescence, a state of irreversible growth arrest that acts as a tumor suppressor mechanism by preventing the replication of damaged cells (16). Short, dysfunctional telomeres are sensed by the cell as DNA double-strand breaks and, thus, trigger the DNA damage response through phosphorylation of the histone H2AX (γ-H2AX) (17). Consistent with its role as a tumor suppressor mechanism, *in vivo* senescence has been detected in pre-malignant lesions but lost in cancers (18). This suggests that senescence markers, such as Dec1, a p53-regulated senescence effector (19), could be useful in assessing cancer risk. Interestingly, senescence also has a tumorigenic effect, as senescent cells secrete a variety of cytokines and other pro-inflammatory proteins that promote tumor progression (20). This intriguing link between senescence and inflammation is currently the subject of active research (21), but little is known of its role in *in vivo* cancer progression.

We postulated that in UC: (1) telomere shortening and DNA damage lead to cellular senescence in pre-neoplastic fields; (2) at some point in the dysplastic sequence, senescence is bypassed to allow tumor progression; (3) chronic inflammation is the underlying mechanism that triggers telomere shortening and senescence in the pre-neoplastic colon of UC patients. We addressed these issues by analyzing telomere length, telomerase, DNA damage, senescence, p53, p16, and inflammation in multiple biopsies from all histological grades collected along the colon of UC patients.

Material and Methods

Patients and samples

This study included multiple biopsies collected from surgically resected colons from 9 UC patients with HGD or cancer (Progressors) and 4 UC patients without dysplasia or cancer (Non- Progressors) (Table 1). The indication for colectomy in UC Progressors was diagnosis of HGD or cancer at colonoscopy, whereas for UC non- Progressors was intractability of symptoms. All patients had at least 8 years of disease duration. For each Progressor, an average of 7 biopsies was analyzed (minimum 5, maximum 10). These biopsies included HGD, LGD, and non-dysplastic biopsies collected at random locations in the colon from each patient. For each biopsy, the position in cm from the rectum was recorded. Colon maps of the histological diagnoses of Progressors are included in Supplementary Fig. 1. For each Non-Progressor, 5 biopsies negative for dysplasia were collected from locations throughout the colon. Controls we included 21 colon biopsies collected at colonoscopy from individuals without UC (non-UC colon). The diagnosis at colonoscopy of the normal controls included diverticulitis, prolapse, constipation, hyperplastic polyps, liposarcoma, impacted fecalith, and normal colon cancer screening. All biopsies were split in thirds: the first third was used for epithelial isolation (see below), the second was lightly fixed in 4% paraformaldehyde and paraffin embedded for immunofluorescence studies, and the last third was frozen for future use. Formalin-fixed, paraffin-embedded biopsies routinely collected at colectomy and matching the locations of the frozen biopsies were used for IHC staining. Samples were collected at the University of Washington Medical Center in Seattle, WA and at the Cleveland Clinic Foundation in Cleveland, OH. These studies were approved by the Human Subjects Review Boards of each institution with annual renewals.

Epithelial cell isolation and DNA extraction

Epithelial cells from frozen biopsies were isolated using epithelial shake-off as previously described (8). Cytokeratin staining confirmed that at least 90% of the cells were epithelial. Epithelial and stromal cells were treated with 1× CHAPS lysis buffer (Chemicon, Billerica, MA) for 30 minutes on ice. After centrifugation, the supernatant, which included the protein extract, was immediately frozen. The pellet was used for DNA extraction with Qiagen DNA extraction kits (Qiagen, Valencia, CA), according to the manufacturer's instructions.

Telomere measurements by Q-PCR

Telomere length was measured by Q-PCR, as previously described (22). Telomeric DNA and a single-copy internal control gene (36B4, acidic ribosomal phosphoprotein PO) were amplified in each sample. The amount of telomeric DNA (T) was divided by the amount of single-copy internal control gene DNA (S), producing a relative measurement of the telomere length (T/S ratio). Two control DNA samples were included in each run to allow for normalization between experiments and periodic reproducibility experiments were performed to guarantee accurate measurements. The intra- and inter-assay variability (coefficient of variation) for Q-PCR was 6 and 7%, respectively.

Telomerase measurement by Q-PCR

Telomerase activity was measured by Q-PCR using a modified protocol of the real-time TRAP assay, as previously described (23). See Supplemental Material for detailed protocol.

γ–H2AX and Dec1 immunostaining

Paraffin-embedded, lightly paraformaldehyde-fixed slides were processed using a modification of previous protocols (11,24). Briefly, after antigen retrieval, slides were stained with a mouse monoclonal anti-phospho-histone H2AX antibody (Ser139) clone

JBW301 (Upstate Biotech, Charlottesville, VA) and rabbit anti-Dec1 (a generous gift from Dr. Adrian Harris). Slides were incubated with secondary antibodies and counterstained (see Supplemental Material for detailed protocol). Images were taken on a Zeiss LSM Meta 510 microscope at 63× with excitation at 543 nm for Alexa 568, 633 nm for Alexa 647, and 405 nm for DAPI, using sequential scans at constant settings for all slides. Images were quantitatively analyzed by calculating the average γ-H2AX and Dec1 staining intensity of at least 100 nuclei per biopsy, in a minimum of 3 fields (25,26).

p53 and p16 immunostaining

Paraffin-embedded, formaldehyde-fixed slides were stained with a mouse monoclonal anti-p53 antibody clone DO-7 (Dako, Carpinteria, CA) or a rabbit polyclonal anti-p16 antibody (Santa Cruz Biotechnology, Santa Cruz, CA) after antigen retrieval. Slides were washed, incubated with secondary antibodies, fixed, counterstained and mounted. Images were acquired with an Olympus BX41 microscope and processed with a Nuance Multispectral Imaging System (CRI, Woburn, MA). This technique allows the deconvolution of the intensities of multiple chromogens by acquiring a spectral absorbance curve at every pixel of the image. The mean density of each chromogen was quantified after segmentation of nuclear or cytoplasmic areas using a watershed algorithm with software developed in our laboratory (26).

Inflammation quantification

Formalin-fixed, paraffin-embedded slides were stained with hematoxylin-eosin and examined under a light microscope. Both chronic and acute inflammation were analyzed. Chronic inflammation was assessed by two different parameters: (1) the presence of infiltrating leukocytes in lamina propria; and (2) the presence of lymphoid aggregates in mucosa and submucosa. Infiltrating leukocytes were quantified using a semi-quantitative scale from 1 to 3, and lymphoid aggregates using a binary scale with 0 for absence and 1 for presence. Acute inflammation was measured using the conventional pathological score for inflammation activity: 0 - inactive, 1 - UC cryptitis; 2 - UC, crypt abcesses; 3 - UC, numerous crypt abcesses; 4 - UC ulcerated and granulation tissue. In a subset of slides, T-cells, B-cells, and macrophages were stained with CD3, CD20, and CD68 antibodies, respectively, using standard immunohistochemistry techniques. They were quantified using a semi-quantitative scale from 1 to 3. Plasma cells were quantified in the same manner from H&E slides.

Statistical analysis

Non-parametric tests were used throughout the studies due to the small number of cases in some groups. In particular, the Mann-Whitney test and the Kruskal-Wallis test were used wherever appropriate to compare the means of quantitative variables in groups defined by qualitative variables. The strength of the associations among quantitative variables was presented by the Spearman's correlation coefficient. Chi-squared tests were used to compare qualitative variables. All the tests were two-sided at an alpha level of 0.05.

Results

The pre-neoplastic field in UC colon expands at least 10cm from dysplasia and cancer

The analysis of multiple biopsies, mostly negative for dysplasia, along the colon of Progressors allowed us to accurately map the molecular and cellular abnormalities studied in relation to their proximity to dysplasia. Detailed colon maps for each of the 9 Progressors are shown in Supplementary Fig.S1. The information derived from biopsies analyzed for non-UC colon, UC Non Progressors, and UC Progressors is summarized in a heat map in

Supplementary Fig.S2, with samples ordered by increasing histologic grade (negative, LGD, and HGD) and by decreasing distance (in cm) to the nearest site of HGD or cancer. One of the most striking observations from this heat map is that shorter telomeres, and higher levels of γ-H2AX, Dec1 and infiltrating leukocytes appeared more prevalent in negative biopsies located less than 10cm from HGD or cancer than in biopsies located further away. For subsequent analyses, we grouped biopsies according to these categories. Fig.1 shows the comparison of means for all the quantitative parameters of the study using this biopsy grouping.

Early UC neoplastic progression is associated with telomere shortening, decreased telomerase activity, increased DNA damage, increased senescence, and reduced expression of p16 and p53

Early UC progression was significantly associated to telomere shortening: a dramatic telomere length decline was observed in colonic epithelium from Progressors compared to Non-Progressors and, for Progressors, between non-dysplastic biopsies away from dysplasia and closer to dysplasia. The shortest telomeres in Progressors were found in LGD biopsies (Fig.1A and Supplementary Table 1). Overall, non-dysplastic biopsies of Progressors had, in average, telomeres that were 22.1% shorter than the telomeres of Non- Progressors (mean ± SD: 1.02±0.18 for Non- Progressors vs. 0.80±0.19 for Progressors; Mann-Whitney p-value <0.0001, Supplementary Table 1). Interestingly, stromal telomere length decreased significantly only between biopsies from UC patients compared to non-UC colon (Fig.1B and Supplementary Table 1). Throughout the neoplastic progression of UC, the telomeres of stroma cells remained unchanged and significantly longer than the telomeres of epithelial cells (mean telomere length ± SD for all UC biopsies measured in stroma 1.10±0.25 vs. 0.84±0.22 measured in epithelium; Mann-Whitney p-value<0.0001).

A significant decrease of telomerase activity was found between Non-Progressor epithelium and Progressor non-dysplastic epithelium that was more than 10cm away from neoplasia (Fig.1C and Supplementary Table 1). Telomerase activity in the stroma was not statistically different between groups (Fig. 1D and Supplementary Table 1).

In addition to shorter telomeres, negative biopsies <10cm to HGD or cancer also showed significantly higher levels of DNA damage, as quantified by γ-H2AX, and senescence, as quantified by Dec1, compared to biopsies located ≥10cm from those dysplastic areas (Fig. 1E and 1F and Supplementary Table 1).

Negative biopsies from UC Progressors showed significantly lower expression levels for p16 and p53 than negative biopsies from UC Non Progressors (Fig. 1G and 1H and Supplementary Table 1). However, there was no difference in the expression levels of either marker between biopsies located less than or more than 10cm from dysplasia. It is important to note that the high expression of p16 and p53 in UC Non Progressors was not statistically significantly different from the levels of the normal controls since some of the normal colons also showed high levels of both markers. The different underlying medical indications for colectomies in those "normal" colons may be the reason for those unexpected positive results.

Late UC neoplastic progression is associated with telomere lengthening, loss of senescence, and increased expression of p16 and p53

While early UC progression was associated with telomere shortening, the pattern reversed in late UC progression, as telomeres lengthened in the transition from LGD to HGD. Telomeres were the shortest in LGD (0.62±0.19), but significantly increased in HGD (0.83±0.21, p=0.039) to a length comparable to non-dysplastic epithelium that is away from

neoplasia (Fig. 1B, Supplementary Table 1). The most likely explanation for this lengthening is reactivation of telomerase. We did observe an increase of epithelial telomerase activity in the transition from LGD to HGD (Fig. 1D), but this difference did not reach statistical significance (Supplementary Table 1).

In addition to telomere lengthening, the later stages of UC neoplastic progression also involved a decrease of senescence, as indicated by the levels of Dec1. Expression of Dec1 was the highest in LGD biopsies (1.30 ± 0.25), but in HGD biopsies decreased to the level of non-dysplastic biopsies away from neoplasia (1.04 ± 0.10, p=0.045) (Fig. 1G and Supplementary Table 1). The expression levels of p16 and p53 progressively increased with progression (Fig 1H and 1I), although the high heterogeneity observed both inter and intra biopsy rendered the comparison of means non-significant (Supplementary Table 1).

Differential associations between telomeres, DNA damage, and senescence in the malignant progression of UC

p16 and p53 expression levels were strongly associated when all UC biopsies (from UC Non Progressors and UC Progressors) were included in the analysis (Table 2). This association remained significant at the different stages of progression, i.e. UC Non Progressors, UC Progressors negative for dysplasia biopsies, and UC dysplastic biopsies (LGD + HGD). In addition, when all UC biopsies were considered, high levels of γ-H2AX were strongly associated with Dec1 and with shorter telomeres. Interestingly, in UC Non Progressors, high levels of γ-H2AX were also associated with increased expression of p16 and p53. However, in non-dysplastic biopsies from UC Progressors, high DNA damage was only associated with increased senescence, but not with p16 or p53. Finally, in UC dysplastic biopsies, longer telomeres were correlated with decreased Dec1, and conversely, with increased p53 expression.

Patients with greater extents of dysplasia have shorter telomeres and more DNA damage in histologically normal biopsies

Based on the previous data, we hypothesized that the frequency of alterations in histologically negative biopsies should be associated with the extent of dysplasia throughout the colon. To test this hypothesis we quantified the percentage of colonic dysplasia, including LGD, HGD and cancer, for each of the 9 Progressors. This percentage ranged from 5.2% to 61.3% of the biopsies collected at colectomy (an average of 109 (min 86, max 134) biopsies per patient). We also examined the correlation of % of dysplasia with the mean value for telomere length, telomerase activity, and, γ-H2AX, Dec1, p16, and p53 expression calculated from all the histologically normal biopsies present in the colon. Overall, patients with greater extents of dysplasia had shorter telomeres (p=0.049, Fig. 2A), more DNA damage (p=0.002, Fig. 2C), and a tendency for more senescence (p=0.076, Fig. 2D) and more p53 expression (p=0.087, Fig. 2F) elsewhere in the colon. This is likely due to the fact that the pre neoplastic field encompasses a larger region in these patients, predisposing them to a higher chance of progression to dysplasia.

Infiltrating leukocytes are strongly associated with neoplastic progression

Fig. 3A-F illustrates the scoring system used for infiltrating leukocytes in the lamina propria. We observed that LGD biopsies and negative biopsies <10cm from dysplasia frequently showed very high levels of infiltrating leukocytes (3+, Fig. 3D-E), which were rarely observed in other biopsies (Fig. 3A-C,F). When we quantified the proportion of biopsies with high levels of infiltrating leukocytes (3+), the association with progression was highly significant (p=0.017, Table 3). Around half of the biopsies in the 10cm pre-neoplastic field and 61% of LGD biopsies showed abundant infiltrating leukocytes, while in the other groups only 20% or less of the biopsies showed this feature. Remarkably, none of the HGD

biopsies had 3+ infiltrating leukocytes. The two additional inflammation parameters assessed in this study, lymphoid aggregates and inflammation activity, did not show any association with UC progression (Table 3).

The striking association between lamina propria infiltrating leukocytes and UC tumorigenesis prompted us to analyze these biopsies for specific subsets of leukocytes. The leukocytes expanding the lamina propria appeared to be a mixture of T-cells, B-cells, macrophages, and plasma cells, and this composition did not differ between biopsies with low or high lamina propria infiltration (Fig. 3G-I: Non-Progressor, low infiltration; Fig. 3J-L: LGD, high infiltration). However, there appeared to be a difference in the location of B-cells and T-cells, which were basal in Non-Progressor biopsies (Fig. 3G-H), but spread out in the mucosa of Progressor biopsies (Fig. 3J-K).

Lamina propria infiltrating leukocytes are associated with shorter telomeres in epithelium and stroma, increased telomerase activity in stroma, higher levels of Dec1 and decreased p53 expression

Next, we explored to what extent the molecular alterations found in the pre-neoplastic field were related to the inflammatory process that underlies this disease. The levels of the six molecular parameters included in this study were compared between UC biopsies with low or high inflammation as defined by the presence of lamina propria infiltrating leukocytes, lymphoid aggregates and the acute inflammation index. Interestingly, the infiltrating leukocytes showed several highly significant associations with molecular parameters (Fig. 4). UC biopsies with high levels of infiltrating leukocytes in lamina propria had significantly shorter telomeres both in epithelium and stroma ($p < 0.0001$ and $p = 0.0001$, respectively; Fig. 4A-B). Moreover, they had increased stromal telomerase activity ($p = 0.027$; Fig. 4D), more senescence as measured by Dec1 levels ($p = 0.006$; Fig. 4F), and a tendency for higher DNA damage ($p = 0.06$; Fig. 4E) and decreased p53 expression ($p = 0.032$; Fig. 4H).

The acute inflammation index and the lymphoid aggregate index only showed significant associations with telomerase activity, for the acute inflammation index the association was in the stroma ($p = 0.037$) and for the aggregate index the association was in the epithelium ($p = 0.013$). None of the other molecular alterations were different for biopsies with inflammation as measured by these two parameters (data not shown).

Discussion

Our results show that, in UC patients, dysplasia arises in a field of inflammation, short telomeres, DNA damage, and senescence, and provide novel in vivo evidence for the role of senescence as a tumor suppressor mechanism. Although telomeres are shorter in non-dysplastic biopsies of UC Progressors compared to Non Progressors, the shortening is more pronounced in the 10cm surrounding HGD or cancer. Within this area, DNA damage (measured by γ-H2AX) and senescence (measured by Dec1) are significantly increased, likely as a consequence of the underlying chronic inflammation, as demonstrated by the abundance of infiltrating leukocytes. Interestingly, LGD biopsies harbor the shortest telomeres and the highest levels of senescence and infiltrating leukocytes, while HGD biopsies display long telomeres, low levels of senescence, and reduced amount of infiltrating leukocytes. This suggests that telomere-induced senescence acts as a tumor suppressor mechanism in LGD, and that this checkpoint is bypassed in HGD, allowing cell proliferation and subsequent cancer. The escape from senescence coincides with the reactivation of telomerase and the lengthening of telomeres, which could be one of the mechanisms that allow the release of the blockade. In addition, HGD biopsies show overexpression of p53 (this study and (27)), which is likely due to the stabilization of mutant p53 protein (28). Short telomeres induce senescence through the activation of p53, thus the loss of this tumor

suppressor allows a permissive environment in which critically short telomeres can generate chromosomal instability and promote tumor progression (29). The loss of functional p53 may also be responsible for the decreased expression of Dec1, as Dec1 is a transcription factor downstream from p53 (19). Thus the decreased levels of Dec1 observed in HGD are concordant with the overexpression of p53.

In addition to p53, the induction of senescence by critically short telomeres also involves the activation of the p16 pathway (30). In this study, however, we did not observe an increase of p53 or p16 in parallel to the shortening of telomeres and the increase of Dec1 in histologically normal biopsies from UC Progressors. On the contrary, the levels of both tumor suppressors were higher in UC Non Progressors than in histologically normal biopsies from Progressors. A possible interpretation is that the pathways of activation of the DNA damage response are functional in UC Non Progressors, but are somehow impaired in UC Progressors. Previous findings of methylation of the p16 promoter (31) and p53 mutations (4) in non-dysplastic biopsies of UC Progressors support this hypothesis. Moreover, in UC Non Progressors γ-H2AX was associated with Dec1, p16 and p53, suggesting the activation of the DNA damage response and subsequent senescence in biopsies with DNA double strand breaks. However, in non-dysplastic biopsies from UC Progressors, there was a strong association between γ-H2AX and Dec1 (both markers are higher closer to dysplasia), but no association of γ-H2AX and Dec1 with p53 and p16. These surprising results might be an indication of additional senescence pathways activated in the presence of a defective DNA damage response in histologically normal biopsies from UC Progressors. The fact that overexpression of Dec1 induces senescence in p53-knockdown cells (19) supports this possibility, but further research is needed to clarify these results.

Another interesting aspect of this study is the association between infiltrating leukocytes in the lamina propria and progression to dysplasia, supporting a connection between inflammation and cancer. We measured two types of inflammation: active and chronic. Active inflammation is the classical pathological index, which is based on the presence of granulocytes in the epithelium. Chronic inflammation refers to the infiltration of leukocytes (mainly lymphocytes) in the lamina propria. Interestingly, we found that chronic inflammation, but not active inflammation, is associated with tumor progression in UC. Moreover, abundant infiltrating leukocytes were associated with shorter telomeres, increased levels of γ-H2AX, increased levels of Dec1, and reduced p53 expression. These results support previous knowledge that tumor infiltrating leukocytes promote tumor growth (32,33) and suggest that this could be due to DNA damage, telomere shortening, and senescence induced by oxidative stress. Indeed, inflammatory cells produce large amounts of reactive oxygen species, which play a fundamental role in UC tumorigenesis (15,34,35).

In spite of accumulating evidence that chronic inflammation contributes to tumor progression in UC, it is still unknown why, while all UC patients have chronic inflammation, only a subset will develop cancer. Individual variation in telomere attrition, DNA damage response, or oxygen free radical scavenging might contribute to that risk. In this regard, this study points to two different, non-exclusive, hypotheses. The first is that UC Non Progressors may be more efficient in mounting an effective DNA damage response than UC Progressors, as previously discussed. The second hypothesis is that UC Non Progressors may be less prone to tumor progression thanks to a higher telomerase activity, which has been reported to protect the cells from oxidative stress (36,37). Both hypothesis merit further investigation from a mechanistic point of view as well as for the potential for p53 and p16 expression and telomerase activity to be useful markers for cancer risk in UC.

While the prevalent view is that chronic inflammation is the initial trigger for tumorigenesis in UC, there is the possibility that inflammation is also a consequence of underlying

senescence, as senescent cells produce a senescence-associated secretory phenotype (SASP) that is pro-inflammatory. Among many other functions of SASP is the recruitment of leukocytes to the tissue (20), which suggests that the abundant infiltrating leukocytes observed in LGD could be a consequence of a high level of senescence in these biopsies. If that were the case, then the high infiltration should diminish as senescence is reduced, as observed in HGD. While senescence acts as a tumor suppressor mechanism, the SASP is tumorigenic, as it modifies the tissue microenvironment to promote tumor progression. Interestingly, we observed that the stroma of biopsies with high infiltration showed significantly shorter telomeres and more telomerase activity than the stroma of biopsies with low infiltration. Moreover, although the proportion of leukocyte subsets did not seem to change with infiltration, their distribution might be affected, as indicated by the observed migration of B-cells and T-cells from the basal layer to the apical surface. Other studies have reported an important role for stromal alterations in UC carcinogenesis (38,39). Nevertheless, the observations reported here are limited because of the small number of samples and need further investigation.

In conclusion, our results support a model in which inflammation, telomere shortening, and high levels of DNA damage activate the induction of senescence in the colon of UC Progressors. Senescence acts as a tumor suppressor mechanism, preventing colonocytes from progressing further than LGD. Eventually some colonocytes bypass senescence, coinciding with the lengthening of telomeres through activation of telomerase and the loss of p53 function. This allows colonocytes with genetic damage to proliferate and progress to HGD and cancer. Further investigation is needed to elucidate the role of p16 and p53 in the induction and further escape of senescence in UC cancer progression.

Supplementary Material

Refer to Web version on PubMed Central for supplementary material.

Acknowledgments

References

1. Brentnall TA. Molecular underpinnings of cancer in ulcerative colitis. Curr Opin Gastroenterol. 2003; 19:64–8. [PubMed: 15699896]

2. Risques RA, Rabinovitch PS, Brentnall TA. Cancer surveillance in inflammatory bowel disease: new molecular approaches. Curr Opin Gastroenterol. 2006; 22:382–90. [PubMed: 16760754]

3. Chai H, Brown RE. Field effect in cancer-an update. Ann Clin Lab Sci. 2009; 39:331–7. [PubMed: 19880759]

4. Brentnall TA, Crispin DA, Rabinovitch PS, et al. Mutations in the p53 gene: an early marker of neoplastic progression in ulcerative colitis. Gastroenterology. 1994; 107:369–78. [PubMed: 8039614]

5. Burmer GC, Rabinovitch PS, Haggitt RC, et al. Neoplastic progression in ulcerative colitis: histology, DNA content, and loss of a p53 allele. Gastroenterology. 1992; 103:1602–10. [PubMed: 1358743]

6. Hussain SP, Amstad P, Raja K, et al. Increased p53 mutation load in noncancerous colon tissue from ulcerative colitis: a cancer-prone chronic inflammatory disease. Cancer Res. 2000; 60:3333–7. [PubMed: 10910033]

7. Willenbucher RF, Aust DE, Chang CG, et al. Genomic instability is an early event during the progression pathway of ulcerative-colitis-related neoplasia. Am J Pathol. 1999; 154:1825–30. [PubMed: 10362807]

8. Rabinovitch PS, Dziadon S, Brentnall TA, et al. Pancolonic chromosomal instability precedes dysplasia and cancer in ulcerative colitis. Cancer Res. 1999; 59:5148–53. [PubMed: 10537290]

9. von Zglinicki T. Oxidative stress shortens telomeres. Trends Biochem Sci. 2002; 27:339–44. [PubMed: 12114022]

10. Risques RA, Lai LA, Brentnall TA, et al. Ulcerative colitis is a disease of accelerated colon aging: evidence from telomere attrition and DNA damage. Gastroenterology. 2008; 135:410–8. [PubMed: 18519043]

11. O'Sullivan JN, Bronner MP, Brentnall TA, et al. Chromosomal instability in ulcerative colitis is related to telomere shortening. Nat Genet. 2002; 32:280–4. [PubMed: 12355086]

12. Rutter M, Saunders B, Wilkinson K, et al. Severity of inflammation is a risk factor for colorectal neoplasia in ulcerative colitis. Gastroenterology. 2004; 126:451–9. [PubMed: 14762782]

13. Cheng Y, Desreumaux P. 5-aminosalicylic acid is an attractive candidate agent for chemoprevention of colon cancer in patients with inflammatory bowel disease. World J Gastroenterol. 2005; 11:309–14. [PubMed: 15637733]

14. O'Connor PM, Lapointe TK, Beck PL, Buret AG. Mechanisms by which inflammation may increase intestinal cancer risk in inflammatory bowel disease. Inflamm Bowel Dis.

15. Roessner A, Kuester D, Malfertheiner P, Schneider-Stock R. Oxidative stress in ulcerative colitis-associated carcinogenesis. Pathol Res Pract. 2008; 204:511–24. [PubMed: 18571874]

16. Ben-Porath I, Weinberg RA. The signals and pathways activating cellular senescence. Int J Biochem Cell Biol. 2005; 37:961–76. [PubMed: 15743671]

17. d'Adda di Fagagna F, Reaper PM, Clay-Farrace L, et al. A DNA damage checkpoint response in telomere-initiated senescence. Nature. 2003; 426:194–8. [PubMed: 14608368]

18. Collado M, Serrano M. The power and the promise of oncogene-induced senescence markers. Nat Rev Cancer. 2006; 6:472–6. [PubMed: 16723993]

19. Qian Y, Zhang J, Yan B, Chen X. DEC1, a basic helix-loop-helix transcription factor and a novel target gene of the p53 family, mediates p53-dependent premature senescence. J Biol Chem. 2008; 283:2896–905. [PubMed: 18025081]

20. Coppe JP, Desprez PY, Krtolica A, Campisi J. The senescence-associated secretory phenotype: the dark side of tumor suppression. Annu Rev Pathol. 5:99–118. [PubMed: 20078217]

21. Fumagalli M, d'Adda di Fagagna F. SASPense and DDRama in cancer and ageing. Nat Cell Biol. 2009; 11:921–3. [PubMed: 19648977]

22. Risques RA, Vaughan TL, Li X, et al. Leukocyte Telomere Length Predicts Cancer Risk in Barrett's Esophagus. Cancer Epidemiol Biomarkers Prev. 2007; 16:2649–55. [PubMed: 18086770]

23. Ohuchida K, Mizumoto K, Ogura Y, et al. Quantitative assessment of telomerase activity and human telomerase reverse transcriptase messenger RNA levels in pancreatic juice samples for the diagnosis of pancreatic cancer. Clin Cancer Res. 2005; 11:2285–92. [PubMed: 15788678]

24. Herbig U, Jobling WA, Chen BP, Chen DJ, Sedivy JM. Telomere shortening triggers senescence of human cells through a pathway involving ATM, p53, and p21(CIP1), but not p16(INK4a). Mol Cell. 2004; 14:501–13. [PubMed: 15149599]

25. O'Sullivan J, Risques RA, Mandelson MT, et al. Telomere length in the colon declines with age: a relation to colorectal cancer? Cancer Epidemiol Biomarkers Prev. 2006; 15:573–7. [PubMed: 16537718]

26. O'Sullivan JN, Finley JC, Risques RA, et al. Telomere length assessment in tissue sections by quantitative FISH: image analysis algorithms. Cytometry. 2004; 58A:120–31. [PubMed: 15057965]

27. Wong NA, Mayer NJ, MacKell S, Gilmour HM, Harrison DJ. Immunohistochemical assessment of Ki67 and p53 expression assists the diagnosis and grading of ulcerative colitis-related dysplasia. Histopathology. 2000; 37:108–14. [PubMed: 10931232]

28. Yoshida T, Matsumoto N, Mikami T, Okayasu I. Upregulation of p16(INK4A) and Bax in p53 wild/p53-overexpressing crypts in ulcerative colitis-associated tumours. Br J Cancer. 2004; 91:1081–8. [PubMed: 15292938]

29. Artandi SE, Attardi LD. Pathways connecting telomeres and p53 in senescence, apoptosis, and cancer. Biochem Biophys Res Commun. 2005; 331:881–90. [PubMed: 15865944]

30. Smogorzewska A, de Lange T. Different telomere damage signaling pathways in human and mouse cells. Embo J. 2002; 21:4338–48. [PubMed: 12169636]

31. Issa JP, Ahuja N, Toyota M, Bronner MP, Brentnall TA. Accelerated age-related CpG island methylation in ulcerative colitis. Cancer Res. 2001; 61:3573–7. [PubMed: 11325821]

32. Allavena P, Garlanda C, Borrello MG, Sica A, Mantovani A. Pathways connecting inflammation and cancer. Curr Opin Genet Dev. 2008; 18:3–10. [PubMed: 18325755]

33. Freund A, Orjalo AV, Desprez PY, Campisi J. Inflammatory networks during cellular senescence: causes and consequences. Trends Mol Med.

34. Itzkowitz SH, Yio X. Inflammation and cancer IV. Colorectal cancer in inflammatory bowel disease: the role of inflammation. Am J Physiol Gastrointest Liver Physiol. 2004; 287:G7–17. [PubMed: 15194558]

35. Seril DN, Liao J, Yang GY, Yang CS. Oxidative stress and ulcerative colitis-associated carcinogenesis: studies in humans and animal models. Carcinogenesis. 2003; 24:353–62. [PubMed: 12663492]

36. Indran IR, Hande MP, Pervaiz S. Tumor cell redox state and mitochondria at the center of the non-canonical activity of telomerase reverse transcriptase. Mol Aspects Med. 31:21–8. [PubMed: 19995569]

37. Saretzki G. Telomerase, mitochondria and oxidative stress. Exp Gerontol. 2009; 44:485–92. [PubMed: 19457450]

38. Matsumoto N, Yoshida T, Okayasu I. High epithelial and stromal genetic instability of chromosome 17 in ulcerative colitis-associated carcinogenesis. Cancer Res. 2003; 63:6158–61. [PubMed: 14559796]

39. Yagishita H, Yoshida T, Ishiguro K, Numata Y, Okayasu I. Epithelial and stromal genetic instability linked to tumor suppressor genes in ulcerative colitis-associated tumorigenesis. Scand J Gastroenterol. 2008; 43:559–66. [PubMed: 18415748]

Abbreviations

γ–H2AX	phosphorylated H2AX
Q-FISH	quantitative fluorescence in situ hybridization
Q-PCR	quantitative PCR
UC	ulcerative colitis
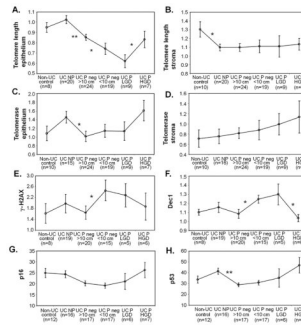
Figure 1.
Comparison of means by histological grade. Error bars indicate standard errors of the mean
(sem). **A:** epithelial telomere length; **B:** stromal telomere length; **C:** epithelial telomerase
activity; **D:** stromal telomerase activity; **E:** γ-H2AX; **F:** Dec1, **G:** p16; and **H:** p53. *
p<0.05, ** p<0.005, based on Mann-Whitney tests.
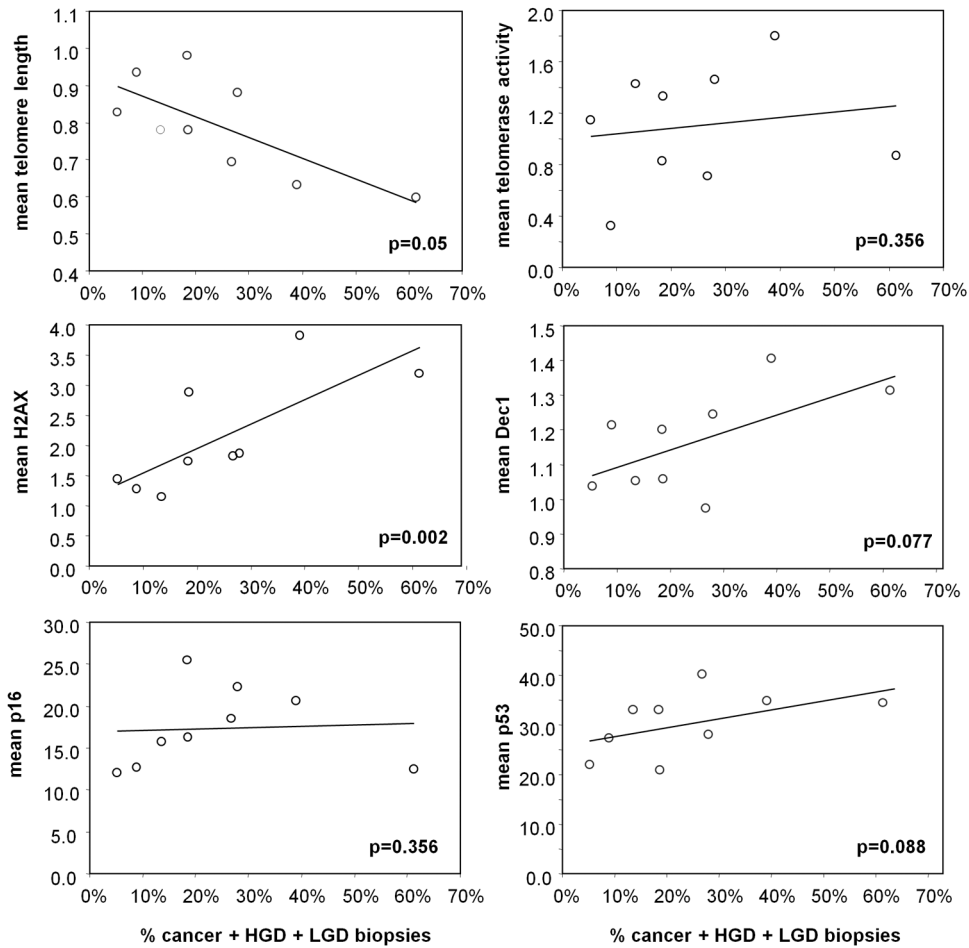
Figure 2.
Correlation between the percentage of dysplasia and the frequency of alterations in histologically negative biopsies for each UC progressor. **A:** epithelial telomere length; **B:** telomerase activity; **C:** γ-H2AX; **D:** Dec1; **E:** p16; and **F:** p53. p-values correspond to the Spearman's correlation coefficient.
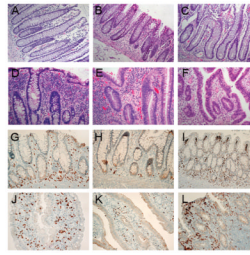
Figure 3.
A-F: Scoring system used for infiltrating leukocytes based on H&E staining. **A:** non UC colon, 1+; **B:** non progressor, 2+; **C:** negative ≥10cm from HGD/cancer, 2+; **D:** negative <10cm from HGD/cancer, 3+; **E:** LGD, 3+; **F:** HGD, 2+. **G-L:** IHC staining from colon of a UC non progressor **(G-I)** and a LGD biopsy from a UC progressor **(J-L)**. **G,J:** T-cells (CD3); **H,K:** B-cells (CD20); **I-L:** macrophages (CD68). 400×.
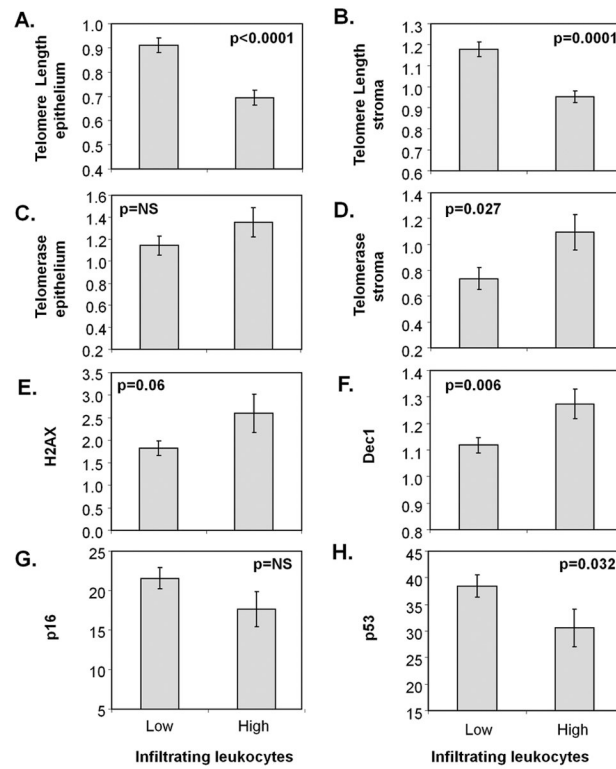
Figure 4.
Association between lamina propria infiltrating leukocytes and **A:** epithelial telomere length, **B:** stromal telomere length, **C:** epithelial telomerase, **D:** stromal telomerase, **E:** γ-H2AX, **F:** Dec1, **G:** p16, and **I:** p53. p-values correspond to Mann-Whitney tests.

Table 1

Ulcerative colitis patients and biopsies included in the study

Patient's highest dysplasia	Age (years)	Disease duration (years)	Disease activity	Total number of biopsies*	≥10cm to HGD or cancer[†]	<10cm to HGD or cancer[†]	LGD	HGD
Non Progressors								
Negative	23	8	mild	5				
Negative	46	17	inactive	5				
Negative	51	20	severe	5				
Negative	52	18	inactive	5				
Total				*20*				
Progressors (most advanced overall diagnosis)								
HGD	32	16	severe	5	3	1	0	1
HGD	34	17	severe	5	2	2	1	0
HGD	36	11	NA	8	4	2	2	0
HGD	48	10	mild	10	6	2	1	1
HGD	58	29	mild	7	3	2	1	1
Cancer	33	13	mild	6	2	2	1	1
Cancer	33	22	NA	5	0	3	1	1
Cancer	36	8	severe	7	4	1	1	1
Cancer	51	13	severe	6	0	4	1	1
Total				*59*	*24*	*19*	*9*	*7*

*
collected throughout the colon,

[†]
negative for dysplasia biopsies located either ≥ or < 10cm from HGD or cancer

Abbreviations:LGD, low grade dysplasia; HGD: high grade dysplasia; NA: not available

Table 2

Spearman correlation coefficient (with p-value) between parameters measured in UC epithelium

	ALL UC biopsies	UC NP	UC progressor negative for dysplasia biopsies	UC dysplasia (LGD+HGD)
Telomere length vs. telomerase	-0.108 (0.329)	-0.193 (0.400)	-0.186 (0.230)	0.034 (0.892)
Telomere length vs. Dec1	-0.176 (0.139)	-0.236 (0.257)	-0.158 (0.362)	**-0.587 (0.051)**
Telomere length vs. γH2AX	**-0.250 (0.033)**	**-0.42 (0.040)**	-0.124 (0.474)	-0.322 (0.286)
Telomere length vs.p16	0.229 (0.071)	0.129 (0.633)	0.047 (0.788)	0.440 (0.133)
Telomere length vs. p53	0.225 (0.076)	0.056 (0.837)	-0.218 (0.210)	**0.659 (0.014)**
Telomerase vs.Dec1	0.116 (0.335)	0.700 (0.161)	0.137 (0.308)	-0.105 (0.727)
Telomerase vs. γH2AX	0.045 (0.705)	0.300 (0.548)	-0.031 (0.818)	0.266 (0.378)
Telomerase vs. p16	**0.301 (0.021)**	0.287 (0.366)	0.159 (0.362)	0.423 (0.150)
Telomerase vs. p53	0.087 (0.514)	0.238 (0.457)	-0.099 (0.571)	0.220 (0.471)
Dec1 vs. γH2AX	**0.516 (<0.001)**	**0.516 (0.013)**	**0.564 (<0.001)**	0.105 (0.727)
Dec1 vs. p16	0.086 (0.521)	0.412 (0.113)	0.067 (0.717)	-0.382 (0.247)
Dec1 vs. p53	-0.099 (0.459)	0.444 (0.085)	0.013 (0.943)	-0.355 (0.285)
H2AX vs. p16	0.186 (0.164)	**0.624 (0.010)**	0.083 (0.656)	-0.236 (0.484)
H2AX vs. p53	0.076 (0.571)	**0.497 (0.050)**	0.083 (0.653)	0.036 (0.915)
p16 vs. p53	**0.498 (<0.0001)**	**0.538 (0.037)**	**0.362 (0.037)**	**0.588 (0.041)**

Table 3

Inflammation scores for biopsies

	Infiltrating Leukocytes				Lymphoid Aggregates			Active Inflammation		
	n	Low (1+)	Low (2+)	High (3+)	n	Absent	Present	n	Inactive	Active
UC Non-Progressors	20	0 (0.0%)	16 (80.0%)	4 (20.0%)	20	6 (30.0%)	14 (70.0%)	17	11 (64.7%)	6 (35.3%)
UC Progressors										
Negative ≥ 10 cm to dysplasia	24	3 (12.5%)	18 (75.0%)	3 (12.5%)	21	12 (50.0%)	12 (50.0%)	24	11 (55.0%)	9 (45.0%)
Negative < 10 cm to dysplasia	18	1 (5.6%)	8 (44.4%)	9 (50.0%)	19	8 (42.1%)	11 (57.9%)	19	10 (41.7%)	14 (58.3%)
LGD	8	1 (12.5%)	2 (25.0%)	5 (62.5%)	7	5 (55.6%)	4 (44.4%)	9	4 (44.4%)	5 (55.6%)
HGD	6	1 (16.7%)	5 (83.3%)	0 (0.0%)	6	2 (28.6%)	5 (71.4%)	7	2 (28.6%)	5 (71.4%)
Pearson Chi-square		$p=0.017$				$p=NS$			$p=NS$	